Original Paper *Forma*, **16**, 125–139, 2001

Directional Change and Transformation of Sliding F-actin Analyzed by a Semi-Automatic Image Tracking System

Satoshi HASEGAWA[1,2], Rieko SHIMO[1] and Koshin MIHASHI[1]

[1]*Graduate School of Mathematics, Nagoya University, Chikusa-ku, Nagoya 464-8602, Japan*
[2]*School of Information Culture, Nagoya Bunri University, Inazawa, Aichi 492-8520, Japan*

(Received March 1, 2001; Accepted July 25, 2001)

Keywords: Image Analysis, Pattern Matching, Actin Filament, in vitro Motility Assay, Living Motion

Abstract. We have developed a semi-automatic image tracking system to analyze the longitudinal sliding and transformation of a string-like object. By using this system, we made a moving image analysis on actin filament (F-actin) in an in vitro motility assay. In this assay, F-actin was sliding on the surface under a fluorescent microscope. The tracking system pursues the fluorescent image of F-actin by matching a polygon line model with the video images. In this study, the directional change and the curvatures of the sliding F-actin were statistically analyzed using the data obtained by the tracking system. The simplified sliding motion of the polygon line model was simulated on a computer. By comparing the result of the analysis with that of the simulation, we found that the sliding F-actin has a flexible and compliant nature.

1. Introduction

In vitro motility assay is a useful method to study motile mechanisms of actin-myosin ATPase system (KRON and SPUDICH, 1986; HARADA *et al*., 1987; HUXLEY, 1990; HIGASHI-FUJIME, 1991). In this assay, actin filament (fibrous actin: F-actin) moves over a myosin-coated glass surface, in the presence of adenosinetriphosphate (ATP). Fluorescent images of string-like F-actin are observed under a fluorescent microscope. F-actin shows a unidirectional sliding with a complicated transformation, as we also described in our previous report (HASEGAWA and MIHASHI, 2000).

Using this motility assay, the sliding velocity of F-actin in various conditions has been studied (YANAGIDA *et al*., 1985; SELLERS and KACHAR, 1990; UYEDA *et al*., 1990; HORIUCHI and CHACKO, 1995; ODA *et al*., 1996; CUDA *et al*., 1997). Also, various types of methods to obtain the sliding velocity either automatically or manually from the video images of the motility assay were reported (SHIRINSKY *et al*., 1992; WORK and WARSHAW, 1992; BOREJDO and BURLACU, 1992; MARSTON *et al*., 1996; UTTENWEILER *et al*., 2000).

However, a problem was pointed out that the winding of the locus and/or the form of sliding F-actin have certain influences on the velocity measurement. The velocity was

underestimated, if it was obtained by measuring the distance between two points such as centroids of filament images at two different times (UTTENWEILER *et al.*, 2000). Even if the center points (or other points such as anterior or posterior tip ends) of the string-like filament images at two different times were used for the velocity determination, the influence of the winding of the locus remained (HASEGAWA and MIHASHI, 2000). In this report, we demonstrate statistically the influence of the locus on the velocity measurement in Subsec. 3.3. These influences cannot be repaired without the information about the locus of the sliding F-actin.

Moreover, the sliding locus or the form of F-actin itself can indicate the important nature of the sliding F-actin (YAMADA and TAKAHASHI, 1992; NISHIZAKA *et al.*, 1993; SHIKATA *et al.*, 1994; HATORI *et al.*, 1996; HONDA *et al.*, 1999). The elasticity and flexibility have already been examined as the nature of static F-actin (NAGASHIMA and ASAKURA, 1980; KÄS *et al.*, 1994). However, the nature of the sliding F-actin (i.e. F-actin interacting with myosin in the presence of ATP) has not sufficiently been solved. The transformation of the sliding F-actin ought to be researched in detail.

In our previous work (HASEGAWA and MIHASHI, 2000), we processed the video images of a sliding F-actin into binary thin line and described the sliding and the transformation by a color pattern. That method was effective to visualize the sliding character. However, by that method, it was difficult to obtain efficiently a number of data large enough to analyze statistically because of the poor conditions of the images, for example, a low contrast and signal-to-noise (S/N) ratio of fluorescent video microscopy.

In the present work, we have developed a semi-automatic tracking system. In this system, the polygon line that is the shape model of F-actin is adjusted to the fluorescent image of F-actin in each frame of the video image. Although this system is not fully automatic, it enables us to obtain data more efficiently. In addition, this system is superior to other previous methods in respect that the transformation can be measured simultaneously with the sliding velocity. In this paper, we first describe the details of the polygon line model and its two applications: the simplified computer simulation and above-mentioned tracking system. Then, we report the results on the fluctuation of the sliding direction and the transformation of the sliding F-actin, which are analyzed by the tracking system. In addition, we discuss the dynamics of F-actin by comparing the results of the analysis with the artificial data generated by the simplified simulation.

2. Materials and Methods

2.1. In vitro motility assay and video fluorescent microscopy

Actin was extracted from acetone-dried powder of rabbit skeletal muscle and then polymerized into F-actin according to the method of SPUDICH and WATT (1971) with a slight modification as shown by SUZUKI and MIHASHI (1991). The F-actin was labeled with Rhodamine-Phalloidin molecular probes. Myosin was extracted from rabbit skeletal muscle following the method of PERRY (1955), and stored at –80°C according to the method of HARADA *et al.* (1990). After this, heavy meromyosin (HMM) was refined from the stored myosin, following the procedures of OKAMOTO and SEKINE (1985) and KRON *et al.* (1991). The movement of F-actin on the surface-fixed HMM was induced by the addition of ATP in the flow cell of the in vitro assay (KRON *et al.*, 1991). Solutions used

for this study contained 2 mM ATP and 25 μg/mL HMM. The experiment was conducted at a room temperature of approximately 22°C.

The fluorescent images of the sliding F-actin were caught by a charge coupled device (CCD) camera with image intensifier (II) (HAMAMATSU ICCD C2400 with II unit C2400-21). These images were recorded on VHS videotape at the rate of interlacing one frame per 1/30 second by using the video image control system (HAMAMATSU ARGUS-100).

2.2. Polygon line model

We defined the polygon line model in order to describe the form of F-actin observed as fluorescent image. The polygon line model is shown and defined in Fig. 1. This polygon line model was used in two applications. One was the simplified simulation (Subsec. 2.3). The other was the semi-automatic tracking system (Subsec. 2.4).

The polygon line model consists of nodes and segment lines as shown in Fig. 1(a). Nodes are the n–1 points that divide filament into n pieces, plus the two tip ends of the filaments. This makes n+1 nodes named, 0, 1, 2, ..., n from the anterior tip end to the posterior end. Segment lines are straight lines that link two neighbor nodes. The number of the segment lines is n. The condition of the node k (k = 0, 1, 2, ..., n) at time t is expressed by the function $f(k,t)$ as shown in Fig. 1(b). The attributes of the $f(k,t)$ such as location coordinates $x(k,t)$, $y(k,t)$ can be defined on demand. The form and other situations of F-actin at time t is expressed by functions $f(0,t)$, $f(1,t)$, ..., $f(n,t)$. Movement and transformation of F-actin are expressed by the temporal change of these functions initialized as $f(0,0)$, $f(1,0)$, ..., $f(n,0)$.

2.3. A simplified simulation of sliding motion by the polygon line model

We simulated the "simplified sliding motion" on a computer by adding basic conditions to the above-mentioned polygon line model. Conditions added to the simplified simulation are following (1)–(5):

(1) The total length of the filament (L) is constant in time.

(2) The segment length (ds) is constant in both time and position ($ds = L/n$).

(3) The sliding speed (v: the absolute value of the velocity) is constantly ds (equal to the segment length) per unit time interval ($v = ds$).

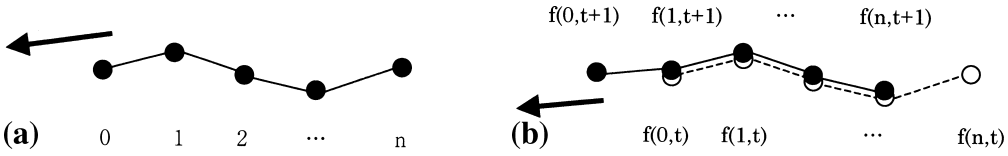

Fig. 1. Polygon line model. This model represents a form of F-actin. (a) Polygon line model consists of nodes and segment lines directly linking neighboring nodes. Nodes represented as dot like black circles were named 0, 1, 2, ..., n from the anterior end to the posterior end. Arrow means sliding direction. (b) Temporal transformation of the polygon line model. Function $f(k,t)$ represents the condition of the node k (k = 0, 1, 2, ..., n) at time t. Locations of the nodes determined by coordinates $x(k,t)$ and $y(k,t)$, or other parameters can be defined as the attributes of the function $f(k,t)$.

(4) Each point of the filament follows the locus of the previous point. In other words, the form of the filament is transported to the back as the sliding occurs. If the initial model is given as $f(0,0)$, $f(1,0)$, $f(2,0)$, ..., $f(n,0)$, then functions $f(1,t)$, $f(2,t)$, ..., $f(n,t)$, except that of anterior tip end $f(0,t)$, are determined as follows:

$$f(n,t) = f(n-1,t-1) \qquad n = 1, 2, \cdots \quad t = 1, 2, \cdots. \tag{1}$$

(5) The function of the anterior tip end $f(0,t)$ that consists of x, y coordinate values is generated according to the following rules:

$$x(0,t) = x(0,t-1) + ds \cdot \cos\theta(0,t) \tag{2.1}$$

$$y(0,t) = y(0,t-1) + ds \cdot \sin\theta(0,t) \tag{2.2}$$

$$\theta(0,t) = \theta(0,t-1) + d\theta \tag{2.3}$$

where $\theta(0,t)$ is the direction from the anterior tip point at time $t-1$ to the one at time t, and $d\theta$ is the directional change of the anterior tip end.

Owing to these five conditions, transformation and movement of polygon lines are all determined by only one parameter of $d\theta$ in the simplified simulation.

We carried out the simplified simulation by giving appropriate initial values to ds and n, and changing the conditions to generate $d\theta$. If $d\theta$ was given as a random number uniformly distributed in ±180°, anterior tip moved randomly and the form of the filament agreed with the locus of the "random walk". This is evidently different from the actual sliding movement. When the distribution of the given random number was limited to approximately ±30°, unidirectional sliding movement was observed in the simulation. Moreover, by giving $d\theta$ in a random number with a normalized distribution $N(0,\sigma)$, the polygon line slid smoothly like actual F-actin.

However, this simulation in which the sliding movement is simplified considerably, differs in detail from the actual F-actin. We will discuss the differences below, comparing the artificial data generated by this simulation with data extracted from the video images of the actual sliding F-actin by using the semi-automatic tracking system.

2.4. The semi-automatic tracking system by the polygon line model

The semi-automatic tracking system can follow the sliding F-actin in low contrast fluorescent video images by fitting the polygon line model (Subsec. 2.2.) to each frame of the video images. The devices to run this software are a moving image analyzing system (Library Co. Ltd. HIMAWARI-60) and a personal computer (NEC PC-9801). The tracking algorithm consisted of an iteration of following three processes:

(1) Manual setting of the initial model (shown in Fig. 2(a))

This tracking system requires a user to set the initial model which is the polygon line fit to the F-actin in video frame at time $t = 0$. The user gives appropriate value to ds (segment length). In this study, we gave $ds = 10$ dot that is equal to 0.8 μm. The user sets the initial model by clicking the mouse button at the node point. The user decides these locations by

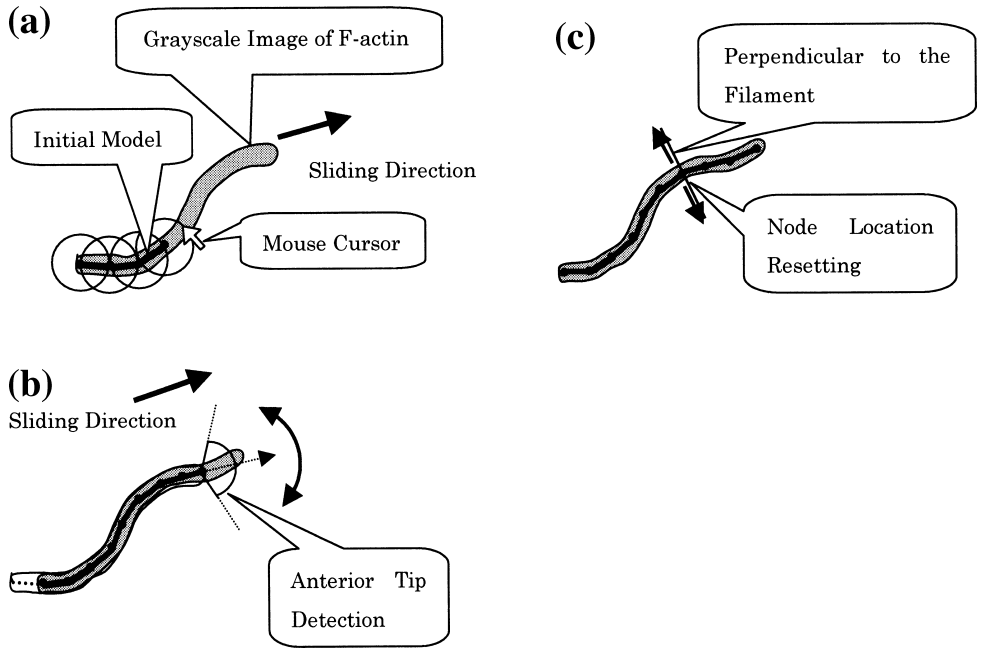

Fig. 2. Concept of the semi-automatic tracking system. (a) Method to set initial polygon line model. At first the posterior end node is located by clicking the computer mouse. Then the circles with a constant radius inputted by user are displayed for every located node to help setting next node. By this method, sequential isometric lines are set as an initial polygon line model. (b) Automatic tracking algorithm. Tracking system searches and detects the anterior tip of a sliding filament automatically by fitting the Gaussian function to the pixel values on an arc whose center is the last anterior tip node. (c) Automatic resetting of the segment model. All nodes are relocated by fitting the Gaussian function to the pixel values on the perpendiculars to the filament.

watching video image. The tracking system supports the user to determine the positions of the nodes, by displaying circles on the video image with uniform radius of *ds* and center of previously determined node (Fig. 2(a)). The value of *n* (number of segment lines) is automatically determined from the number of the nodes set by the user (*n*+1). The initial model, once set, can be saved in a computer file and can be retrieved for the next tracking. All coordinate data of the input initial nodes are integers, however, that will be reset automatically by fitting the Gaussian distribution function into non-integers whose pixel values are calculated by using bilinear interpolation represented as:

$$p(x,y) = (1-a)(1-b)p(X,Y) + a(1-b)p(X+1,Y) + (1-a)bp(X,Y+1) + abp(X+1,Y+1) \quad (3)$$

where $p(x,y)$ is a pixel value at coordinate (x,y). And x and y are non-integers, X, Y are the maximum integer smaller than x, y respectively. Coefficients a and b are $a = x-X$ and $b = y-Y$, respectively.

(2) Automatic search for the anterior tip end (Fig. 2(b))

The moving direction of the anterior tip end of the polygon line model is determined by searching for the new anterior tip end automatically. The new anterior tip end is determined by fitting the Gaussian function into the sequence of pixel values on the arc, of which the center is the previous anterior tip point and the radius is *ds* (shown in Fig. 2(b)). The angle of the arc is $\theta(0,t) \pm w°$, where w is the angle width set by the user. In this study, we set w wide enough to track the movement for each filament image. Most of the values of w were within the range of approximately 30~40°. In this study, the smallest frame interval to detect the anterior tip end was 5/30 second. The appropriate time interval to find a new anterior tip end depends on *ds* and the sliding speed. However, the speed is not necessarily known at the time when this tracking is applied. Thus the above-mentioned detection of the anterior tip end is completed once in every frame. After that, the average brightness on the detected provisional anterior tip segment is compared with the one on the last posterior segment. If the brightness is stronger in the provisional anterior segment than in the posterior segment, then the anterior tip is determined to be a new anterior tip end in this system. This is the method to move a polygon line model forward.

(3) Automatic resetting of the segment model (Fig. 2(c))

The peak of the values is extracted at every node in every frame by fitting Gaussian function to the sequential pixels on the perpendicular to the filament length axis (Fig. 2(c)).

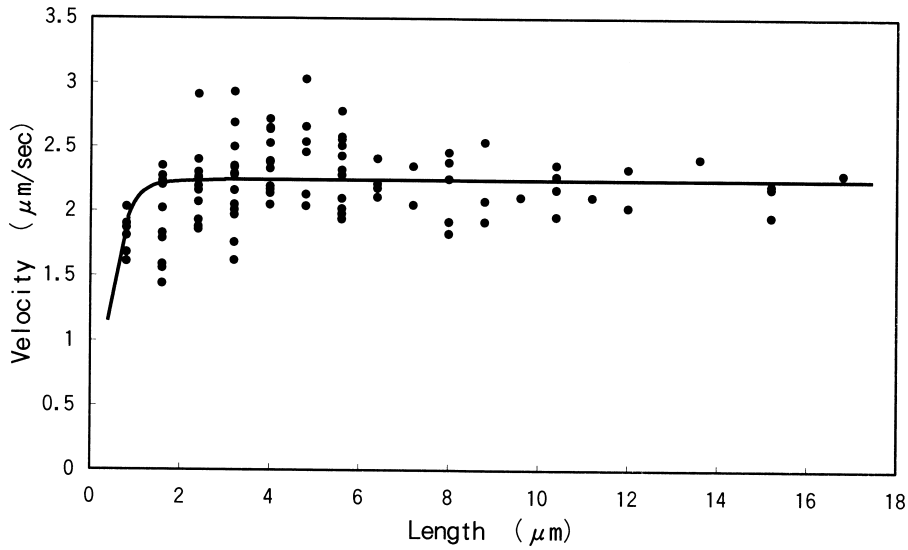

Fig. 3. Dependence of sliding velocity on filament length measured by the semi-automatic tracking system. Velocity is a mean value averaged over the sample number that corresponds to the number of the sequential frames tracked by the system. Each speed was calculated from distances between the anterior tip nodes of polygon line models in two different times. The time interval used to determine each velocity was 2/3 sec. Filament length was a total length of the straight segments of polygon line. 98 points were plotted, which were selected from obtained data of 156 F-actin, so that all of them have a sample number greater than 30. Then the sample number was distributed from 31 to 137.

(This perpendicular is a bisector of the interior angle between two neighboring segments.) By this refitting process, locations of every node on the polygon line are determined with sub-pixel accuracy. These pixel values at the non-integer coordinate are calculated by bilinear interpolation according to the Eq. (3).

3. Results

The time sequences of the coordinate values of the nodes on the polygon line fitted to 156 different F-acin filaments were used in this study. They were obtained under the same experimental conditions mentioned in Subsec. 2.1.

3.1. Sliding velocity as functions of total length of F-actin

Figure 3 shows the sliding velocity (absolute value of the velocity) of F-actin filaments. Each data point corresponded to one F-actin. The sliding velocity was calculated for each F-actin by averaging the instantaneous speeds of the anterior tip node over sample number. Each sample number depends on the length of the time sequence of the successful tracking. The instantaneous speed in the time sequence was measured in every 2/3 second (i.e. 4 frame intervals of 5/30 second). The data that had a sample number greater than 30 were plotted. Values of the total length of individual F-actin were equal to the segment number multiplied by 0.8 μm (=*ds*). The sliding velocity was independent of the filament length up to 17 μm.

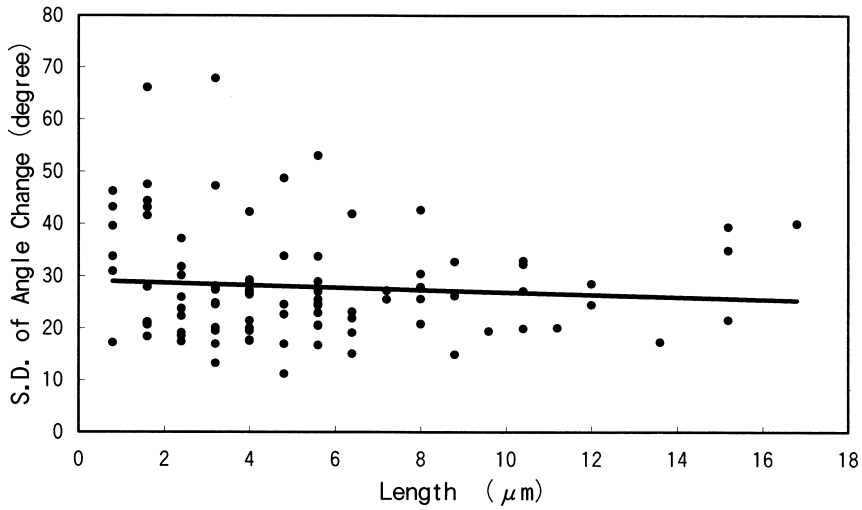

Fig. 4. Dependence of angle fluctuation of the sliding direction on the filament length. Angle fluctuation is represented by the s.d. of the angle change of anterior tip end calculated from locations of anterior tip node of polygon line model in three different times. Filament length is a total length of the straight segments of the polygon line model set in the semi-automatic tracking system. Time interval was 2/3 sec. 98 points in which the data had a sample number greater than 30 were plotted.

3.2. Directional change as functions of total length of F-actin

In Fig. 4, the standard deviations (s.d.) of the time sequence of $d\theta$ calculated over 2/3 second intervals, which indicated fluctuations of sliding directions of individual F-actin, were shown as a function of the total length of F-actin. Fluctuations in the sliding direction of the shorter F-actin were more significant than the long F-actin. There appeared only a small negative dependence of the directional fluctuation on the filament length, though the previous report by SHIKATA *et al.* (1994) showed a large dependence on the filament length. The reason for this discrepancy was not clear.

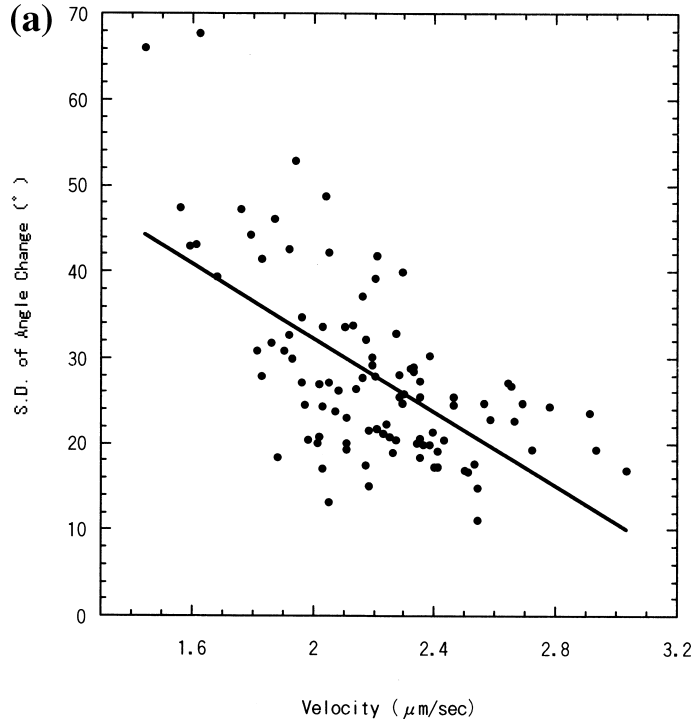

Fig. 5. Dependence of fluctuation of the sliding direction or angle of the anterior tip portion on the sliding velocity. (a) Angle fluctuation of sliding direction versus velocity of actual sliding F-actin. Velocity is a mean value of the speeds determined by the semi-automatic tracking system with the time interval of 2/3 sec. Angle fluctuation of sliding direction is s.d. of the directional change calculated from the anterior tip locations at three different times. (b) Angle fluctuation of the sliding direction versus velocity of the computer simulation of the moving polygon line. Values were calculated with the same method used in (a). (c) Angle fluctuation of the anterior tip segment (~0.8 μm from the anterior tip) versus velocity of actual sliding F-actin. Angle fluctuation of anterior tip segment was s.d. of the angle change of the anterior one segment in polygon line calculated from angles at two different times. Time interval was 2/3 second in both (a) and (c). The time interval in the case (b) was 6 frames, where the unit interval of the simulation was 1 frame. The number of the plotted data is 98 points in (a) and (c), and 96 in (b). Plotted data were selected so that they had a sample number greater than 30.

3.3. Changes in the sliding direction and the angle of the anterior tip segment

The influence of the sliding locus on the velocity measurement is shown statistically, based on the actual sliding (Fig. 5(a)) and the simulation (Fig. 5(b)). In addition, by comparing Fig. 5(c) with Fig. 5(a), a curious result on the anterior portion of actual F-actin will be demonstrated below.

Figure 5(a) shows a relationship between the sliding velocity (the same values as the ordinate in Fig. 3) and the fluctuation of the sliding direction (the same as the ordinate in Fig. 4). Negative correlation is shown in Fig. 5(a). However, it would be incorrect to understand that the negative correlation (in Fig. 5(a)) indicates a physical phenomenon such that the increase of the velocity limits the fluctuation of the sliding direction. Such a conclusion is drawn from a misinterpretation of the 'velocity' that was computed by dividing the length of the vector connecting the anterior tip points in two different frames by the time interval between frames. This velocity was underestimated owing to the winding of the sliding locus (HASEGAWA and MIHASHI, 2000). This 'velocity' distribution represents a degree of the winding in the locus rather than the difference in actual sliding speed.

In fact, the negative correlation between this 'velocity' and fluctuation of direction is also shown in Fig. 5(b). This is the case of the simplified simulation (mentioned in Subsec. 2.3), in which the polygon lines moved without any physical influence. The sliding velocity

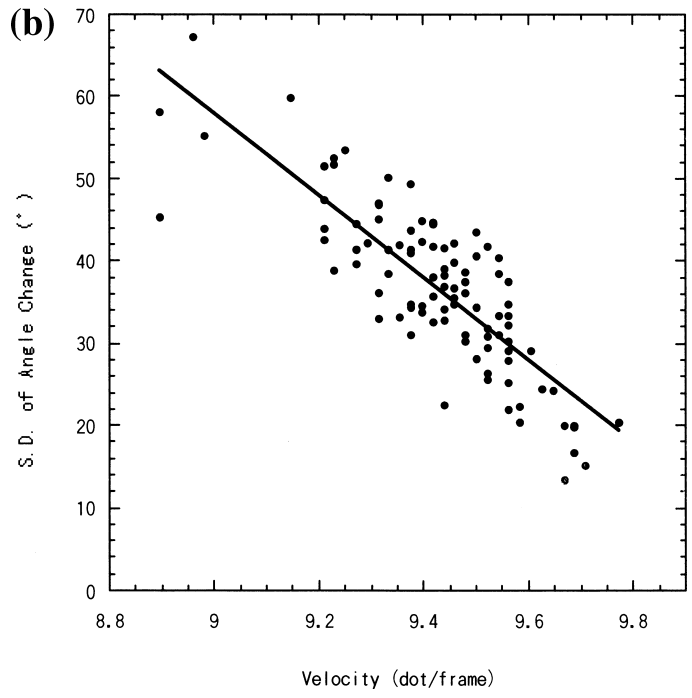

Fig. 5. (continued).

given for each unit time-interval was constant. However, the 'velocity' computed from the artificial data is varied depending on the winding of the sliding locus, when it was computed with the time-interval larger than the unit interval (Fig. 5(b)). Therefore, the negative correlation shown in Fig. 5(a) should also illuminate only a simple fact that the fluctuation of sliding direction depends on the winding of the sliding locus.

In contrast, the tendency shown in Fig. 5(c) is different from Figs. 5(a) and 5(b). In the case of Fig. 5(c), abscissa is the same as the case of Figs. 5(a) and 5(b), but the ordinate is s.d. of the angle change of the anterior one segment (~0.8 μm from anterior tip) in the polygon line models fitted to the images of the actual F-actin. The angle change was calculated with the same time interval of 2/3 second as the case of 5(a). In this case (Fig. 5(c)), the angle change of the anterior tip segment was independent of the winding of the sliding locus.

In the simplified simulation, the angle of the anterior tip segment was equal to the sliding direction, and both of them deeply depended on the winding of the sliding locus as shown in Fig. 5(b). This is one of the differences between the simplified simulation and the actual sliding F-actin.

3.4. Curvature distribution along the longitudinal axis of F-actin

Of sliding F-actin, the mean curvatures varied along the longitudinal axis of F-actin

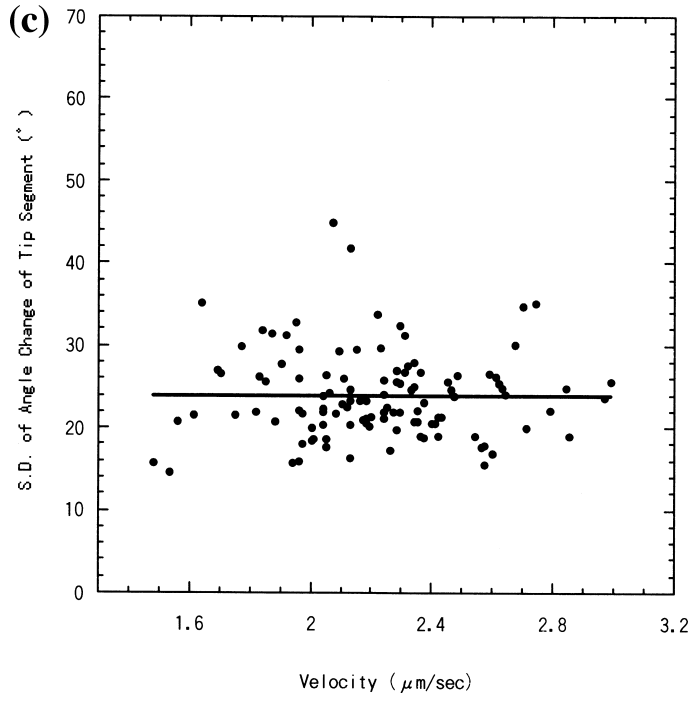

Fig. 5. (continued).

(Fig. 6). The mean curvatures of F-actin were calculated as $(<\kappa^2>)^{1/2}$, where κ (being the curvature computed from the coordinates of three neighboring nodes and the brackets < > denoting the average over obtained data. The mean curvature at the points of each node was calculated, except the anterior and posterior tip nodes, and shown in Fig. 6 as a function of the distance from the anterior node. We see that (1) the maximum value of the mean curvatures of F-actin increased as the length of the filament increased. (2) In shorter filaments (shorter than ~4 μm approximately), the mean curvatures were almost constant along the longitudinal axis. (3) In longer filaments (longer than ~4 μm approximately), the mean curvature increased as the distance from the anterior tip end increased, excepting the anterior tip portion (~2 μm from the anterior tip end) and the posterior tip portion (~1 μm from the posterior tip end). These suggested that the curvature of filament tended to accumulate in the direction of the posterior tip.

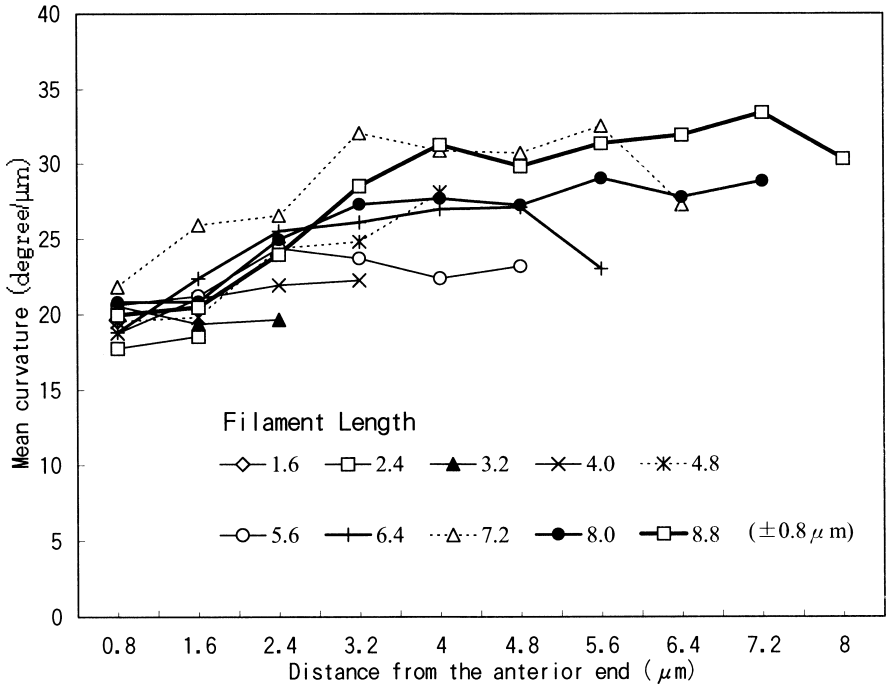

Fig. 6. Regional distribution of mean curvatures on sliding F-actin. The node interval of the fitted polygon line was ~0.8 μm (ds = 10 dot). The curvatures are the angle change per 1 μm, calculated from coordinates of three neighboring nodes. Mean curvatures are ordered along the abscissa, from the anterior node to the posterior node points, except the anterior and posterior tip nodes. Plotted 10 lines are the data of the polygon line that have 3–12 nodes (i.e. 2–11 segments), they are equal to the filament length of 1.6 ± 0.8 μm ~ 8.8 ± 0.8 μm, respectively. These mean curvatures were the averages of 856 (18), 898 (16), 883 (18), 870 (17), 425 (10), 785 (14), 544 (12), 276 (7), 439 (8) and 254 (5) samples respectively, where the numbers shown inside the parentheses are the number of the F-actin tracked by the tracking system.

4. Discussions

4.1. Analysis by the semi-automatic tracking system

It is a well-known observation that the sliding velocity of F-actin in an in vitro motility assay is independent of the length of F-actin (YANAGIDA *et al.*, 1985; HARADA *et al.*, 1990; TOYOSHIMA *et al.*, 1990; UYEDA *et al.*, 1990). This was verified in the present study by utilizing the semi-automatic tracking system as shown in Fig. 3. However our study also showed that a large variety of the sliding speed appeared in the shorter filaments. One of the reasons why the velocity of the shorter filament varied is probably due to a large variety of the sliding locus. The 'velocity' was influenced by the winding of the sliding locus as shown in Fig. 5(a). The tracking system introduced in this study made it possible to analyze the locus and form of sliding F-actin efficiently as well as the velocity. However, this system was not fully automatic with respect to that the users have to set initial model manually and to judge whether the tracking is successful or not. The tracking would fail when the images of more than two filaments crossed each other during the sliding. It also fails when quality of the images such as contrast or S/N ratio was poor in sequential video frames. It therefore remains to be refined.

4.2. Nature of sliding F-actin

By comparing the results of the simplified simulation with that of the actual sliding, we understood the characteristics of sliding F-actin. In the simplified simulation (in Subsec. 2.3), it is assumed that the sliding velocity is independent of the filament length. This explained the observations of the actual F-actin (Fig. 3). It was also shown equally in both the simulation (Fig. 5(b)) and the actual sliding (Fig. 5(a)), that the fluctuation of sliding direction depended on the winding of the sliding locus.

On the contrary, the differences between the simplified simulation and the actual sliding appeared in following three points.

(1) Dependence of the directional change on the filament length

It was assumed in the simplified simulation that the directional change is independent of the filament length. However, a weak negative dependence appeared in the actual F-actin (Fig. 4). SHIKATA *et al.* (1994), predicted that fluctuation in the sliding direction $d\theta$ depends on the filament length L in a manner of $d\theta \propto L^p$, where p was a parameter representing the nature of sliding F-actin. If the sliding object was a rigid straight bar, then the directional fluctuation $d\theta$ would be inversely proportional to the length taking $p = -1$. If, on the other hand, the sliding object was semi-flexible, then $-1 < p < 0$. The result obtained by SHIKATA *et al.* (1994) indicated that $p = -0.7$ approximately. This meant that F-actin retained its semi-flexibility during sliding motion. The result we obtained (Fig. 4), however, showed that p was nearly 0 ($p < 0$). In the previous study (SHIKATA *et al.*, 1994), the conditions of the running solution in the motility assay were different. For instance, there were not only ATP but also GTP present in the solution. Therefore, discrepancy between two studies may not simply be attributed to difference in the nature of F-actin. The value of p we found was nearly 0 ($p < 0$). This corresponded to a highly compliant nature of the sliding F-actin particularly in bending motion. If p equals really 0, it means that the sliding F-actin is completely compliant and no interrelation exists between the sliding

direction and the posterior portion of the F-actin. In other words, if $p = 0$, the sliding direction of the anterior tip end was generated by only the anterior tip itself and was independent of the posterior portion as in the case of the simplified simulation. However, in the actual F-actin, p was less than zero.

(2) Behavior of the anterior portion

In the simplified simulation, the sliding direction of the anterior tip end was exactly equal to the angle of the anterior one segment, and its temporal change ($d\theta$ in Eq. (2.3)) was also the same. Therefore, the fluctuation of both $d\theta$ depended equally on the winding of sliding locus as shown in Fig. 5(b). In actual sliding F-actin, however, dependence was shown only in the case of the sliding direction (Fig. 5(a)). The angle of the anterior segment was independent of the locus (Fig. 5(c)). This fact suggested that the anterior ~1 μm portion of actual F-actin moved in a different manner from the change of the sliding direction. Possible nature of the sliding F-actin that was responsible for such behavior of the anterior portion will be discussed below.

(3) Distributions of the curvatures along the long axis of filament.

In the simplified simulation, curvatures in the polygon line are also generated only by $d\theta$ (in Eq. (2.3)), and the mean curvatures are independent of both filament length and the position in a filament.

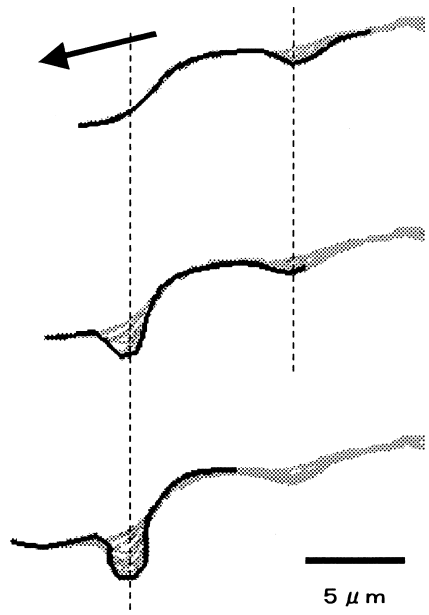

Fig. 7. An example of the transformation of a sliding F-actin. These are displayed by computer graphics using the coordinate data of the nodes in the polygon line obtained by matching them to the video image by the semi-automatic tracking system. Typical scenes to show the growth of the buckling are selected in this figure. Arrow indicates the sliding direction.

However, in the actual F-actin, it was often observed that the curvature was generated and grown in the middle portion of F-actin during sliding as depicted in Fig. 7. Statistical analysis, shown in Fig. 6, also suggested the growing of the curvatures and its transfer to the direction of the posterior part. This tendency corresponded to actual observations that the buckling of filament was occurred and gradually increased (as shown in Fig. 7). In short filaments, the mean curvatures of filament were limited in small values (Fig. 6). It was also limited in small values in the tip portions of the long filaments (Fig. 6). These small mean curvature may be due to the high elasticity of the sliding F-actin. It is reasonable that quick release of the buckling might occur at the open ends of the filament. This release may also generate the fluctuation of the angle in the anterior portion that does not agree with the change of the sliding direction or the winding of the sliding locus (as shown in Fig. 5(c) and discussed above).

Taking the above statements (1)–(3) into consideration, the transformation of the fluorescent image of F-actin indicated the elasticity and compliance of sliding F-actin. The verification of the influence of this nature on the mechanisms of the sliding movement is up to the future elucidation of the more detailed structure transformation of F-actin as well as the energy transfer mechanisms related to myosin and ATPase activity.

We thank Dr. Hajime Honda (Nagaoka University of Technology) and Dr. Kenji Oosawa (Nagoya University) for their encouragement and useful discussions. We are grateful to Mr. Kenichi Izumi, Mr. Masahiro Hasegawa and other members of Mihashi's laboratory for their critical discussions. We also thank Mr. Paul Legé for his advice on English.

REFERENCES

BOREJDO, J. and BURLACU, S. (1992) Velocity of movement of actin filaments in vitro motility assay. Measured by fluorescence correlation spectroscopy, *Biophys. J.*, **61**, 1267–1280.

CUDA, G., PATE, E., COOKE, R. and SELLERS, J. R. (1997) In vitro actin filament sliding velocities produced by mixtures of different types of myosin, *Biophys. J.*, **72**, 1767–1779.

HARADA, Y., NOGUCHI, A., KISHINO, A. and YANAGIDA, T. (1987) Sliding movement of single actin filaments on one-headed myosin filaments, *Nature*, **326**, 805–808.

HARADA, Y., SAKURADA, K., AOKI, T., THOMAS, D. D. and YANAGIDA, T. (1990) Mechanochemical coupling in actomyosin energy transduction studied by in vitro movement assay, *J. Mol. Biol.*, **216**, 49–68.

HASEGAWA, S. and MIHASHI, K. (2000) Analysis of sliding actin filaments utilizing a novel method of spatiotemporal color patterns, *Forma*, **15**, 377–391.

HATORI, K., HONDA, H. and MATSUNO, K. (1996) ATP-dependent fluctuations of single actin filaments in vitro, *Biophys. Chem.*, **58**, 267–272.

HIGASHI-FUJIME, S. (1991) Reconstitution of active movement in vitro based on the actin-myosin interaction, *Int. Rev. Cytol.*, **125**, 95–138.

HONDA, H., HATORI, K., IGARASHI, Y., SHIMADA, K. and MATSUNO, K. (1999) Contractile and protractile coordination within an actin filament sliding on myosin molecules, *Biophys. Chem.*, **80**, 139–143.

HORIUCHI, K. Y. and CHACKO, S. (1995) Effect of unphosphorylated smooth muscle myosin on caldesmon mediated regulation of actin filament motility, *J. Muscle Res. Cell Motil.*, **16**, 11–19.

HUXLEY, H. E. (1990) Sliding filaments and molecular motile systems, *J. Biol. Chem.*, **265**, 8347–8350.

KÄS, J., STREY, H. and SACKMANN, E. (1994) Direct imaging of reptation for semiflexible actin filaments, *Nature*, **368**, 226–229.

KRON, S. J. and SPUDICH, J. A. (1986) Fluorescent actin filaments move on myosin fixed to a glass surface, *Proc. Natl. Acad. Sci. U.S.A.*, **83**, 6272–6278.

KRON, S. J., TOYOSHIMA, Y. Y., UYEDA, T. Q. P. and SPUDICH, J. A. (1991) Assays for actin sliding movement over myosin-coated surfaces, *Method Enzymol*., **196**, 399–416.

MARSTON, S. B., FRASER, I. D. C., BING, W. and ROPER, G. (1996) A simple method for automated tracking of actin filaments in the motility assay, *J. Muscle Res. Cell Motil*., **17**, 497–506.

NAGASHIMA, H. and ASAKURA, S. (1980) Dark-field light microscopic study of the flexibility of F-actin complexes, *J. Mol. Biol*., **136**, 169–182.

NISHIZAKA, T., YAGI, T., TANAKA, Y. and ISHIWATA, S. (1993) Right-handed rotation of an actin filament in an in vitro motile system, *Nature*, **361**, 269–271.

ODA, T., SHIKATA, Y. and MIHASHI, K. (1996) Mutual sensitization of ATP and GTP in driving F-actin on the surface-fixed H-meromyosin, *Biophys. Chem*., **61**, 63–72.

OKAMOTO, Y. and SEKINE, T. (1985) A streamlined method of subfragment one preparation from myosin, *J. Biochem*., **98**, 114–1145.

PERRY, S. V. (1955) Myosin adenosinetriphosphatease. ATP + $H_2O \rightarrow$ ADP + H_2PO_4, *Methods Enzymol*., **2**, 582–588

SELLERS, J. R. and KACHAR, B. (1990) Polarity and velocity of sliding filaments: control of direction by actin and of speed by myosin, *Science*, **249**, 406–408.

SHIKATA, Y., SHIKATA, A., SHIMO, R., TAKADA, H., KATO, C., ITO, M., ODA, T. and MIHASHI, K. (1994) Statistical Analysis on the Angle Fluctuation of the Direction of a Single F-actin Sliding on the surface-fixed H-meromyosin, *Proc. Japan Acad*., **B70**, 117–120.

SHIRINSKY, V., BIRUKOV, K. G., HETTASCH, J. M. and SELLERS, J. R. (1992) Inhibition of the relative movement of actin and myosin by caldesmon and calponin, *J. Biol. Chem*., **267**, 15886–15892.

SPUDICH, J. A. and WATT, S. (1971) The regulation of rabbit skeletal muscle contraction. I. Biochemical studies of the tropomyosin-troponin complex with actin and the proteolytic fragments of myosin, *J. Biol. Chem*., **246**, 4866–4871.

SUZUKI, N. and MIHASHI, K. (1991) Binding mode of cytochalasin *B* to F-actin is altered by lateral binding of regulatory proteins, *J. Biochem*., **109**, 19–23.

TOYOSHIMA, Y. Y., KRON, S. J. and SPUDICH, J. A. (1990) The myosin step size: measurement of the unit displacement per ATP hydrolyzed in an in vitro assay, *Proc. Natl. Acad. Sci. U.S.A*., **87**, 7130–7134.

UTTENWEILER, D., VEIGEL, C., STEUBING, R., GÖTZ, C., MANN, S., HAUSSECKER, H., JÄHNE, B. and FINK, R. H. A. (2000) Motion determination in actin filament fluorescence images with a spatio-temporal orientation analysis method, *Biophys. J*., **78**, 2709–2715.

UYEDA, T. Q. P., KRON, S. J. and SPUDICH, J. A. (1990) Myosin step size estimation from slow sliding movement of actin over low densities of heavy meromyosin, *J. Mol. Biol*., **214**, 699–710.

WORK, S. S. and WARSHAW, D. M. (1992) Computer-assisted tracking of actin filament motility, *Anal. Biochem*., **202**, 275–285.

YAMADA, A. and TAKAHASHI, K. (1992) Sudden increase in speed of an actin filament moving on myosin cross-bridges of "mismatched" polarity observed when its leading end begins to interact with cross-bridge of "matched" polarity, *J. Biochem*., **111**, 676–680.

YANAGIDA, T., ARATA, T. and OOSAWA, F., (1985) Sliding distance of actin filament induced by a myosin crossbridge during one ATP hydrolysis cycle, *Nature*, **316**, 366–369.